

## Simulation and Experimental Studies on Proton Diffusion in Polyelectrolytes Based on Sulfonated Naphthalenic Copolyimides

Leoncio Garrido,<sup>†</sup> Javier Pozuelo,<sup>‡</sup> Mar López-González,<sup>†</sup> Jianhua Fang,<sup>§</sup> and Evaristo Riande<sup>\*,†</sup>

<sup>†</sup>Departamento de Química Física, Instituto de Ciencia y Tecnología de Polímeros (CSIC), 28006 Madrid, Spain, <sup>‡</sup>Departamento de Ciencia e Ingeniería de Materiales e Ingeniería Química (IAAB), Universidad Carlos III de Madrid, 28911 Leganés, Spain, and <sup>§</sup>School of Chemistry and Chemical Technology, Shanghai Jiao Tong University, Shanghai 200240, China

Received April 15, 2009; Revised Manuscript Received July 22, 2009

**ABSTRACT:** This work describes proton transport in membranes cast from dimethyl sulfoxide solutions of polyelectrolytes obtained by polycondensation of 4,4'-diaminodiphenyl ether (ODA) and 4,4'-diaminodiphenyl ether-2,2'-disulfonic acid (ODADS) with 1,4,5,8-naphthalenetetracarboxylic dianhydride (NTDA), the moles of sulfonated diamine per mole of unsulfonated one being roughly 3/1. Pulsed field gradient (PFG) NMR studies reveal two kinds of water: water located in the pores of the membranes appearing in the range 5 to 1 ppm and a minor amount of water associated with the imide groups, appearing at 1 ppm. The diffusion coefficient of <sup>1</sup>H in the first type of water is about 2 orders of magnitude higher than that measured in the second type and in both cases the values of this parameter severely decrease as the water content of the membranes decreases. The diffusion coefficients of bare protons, hydronium ions and water in the membranes were calculated using molecular dynamics techniques. For membranes with low water content, the diffusion coefficient of <sup>1</sup>H is very close to the diffusion coefficients of water and hydronium ions obtained by simulation. At high concentrations the simulated values are higher than  $D(^1\text{H})$ . The simulated values obtained for the diffusion coefficients of hydronium ion and water for membranes equilibrated with water are fairly close to those estimated, respectively, from proton conductivity and osmotic measurements. This work suggests that the study of cation-exchange membranes in the acidic form using NMR, conductivity, and molecular dynamics simulation techniques provides useful information on how structure and water content affect transport processes in membranes.

### Introduction

Owing to its excellent conductivity and chemical stability, Nafion is nowadays the most popular polyelectrolyte used to separate the anode from the cathode in low temperature fuel cells.<sup>1,2</sup> However, Nafion presents some drawbacks involving high cost, environmental concerns, limiting working temperature and methanol crossover.<sup>3,4</sup> The information at hand suggests that some of the drawbacks that Nafion presents can be alleviated with inorganic hydrophilic additives such as silica,<sup>5,6</sup> superacid zirconium,<sup>7</sup> and zirconium phosphate,<sup>8</sup> which promote water retention and proton transportation in the composites. A great deal of work has been carried out in recent years searching for alternative materials to Nafion as described in several recent reviews.<sup>9–13</sup> Membranes based on polymers with chemical and thermal stability such as polyether ketones,<sup>14</sup> polysulfones,<sup>15</sup> polyimides,<sup>16</sup> etc., are being investigated as polyelectrolyte for low temperature fuel cells. It has been suggested that multiblock copolymers prepared from disulfonated poly(arylene ether sulfone) and naphthalene polyimide retain humidity at temperatures exceeding 120 °C combined with morphological stability and therefore can be suitable candidates as high temperature polyelectrolyte membranes.<sup>17</sup> This is an important finding because one of the major challenges facing the technology of commercial low temperature fuel cells is to develop polyelectrolytes with both low water content and improving conductivity at low RH.

Each molecular chain in sulfonic acid polyelectrolytes combines hydrophobe moieties with hydrophilic residues containing

the sulfonic acid functional groups. In presence of water the sulfonic acid groups of cation-exchange membranes aggregate giving rise to the nanoseparation of hydrophobic/hydrophilic domains. If the hydrophilic domains form percolation paths, the membrane exhibits high conductivity. The role of water in conductivity is a complex process because water intervenes in the following: (a) dissociation of the acid group, (b) transfer of the proton to the aqueous medium, and (c) screening of the proton from the sulfonate anion and finally diffusion of the proton in the polymer matrix.<sup>18</sup> The mechanisms involved in proton transport across cation-exchange membranes have drawn the attention of many researchers.<sup>18,19</sup> *Ab initio* simulations suggest that the proton state in bulk water and in water clusters<sup>20–24</sup> fluctuates between more localized hydronium ion-like states or Eigen ions and more delocalized H<sub>5</sub>O<sub>2</sub><sup>+</sup>-like states or Zundel ions. Proton diffusion involving this mechanism is named structural diffusion. The proton transport is believed to be the result of forming and breaking hydrogen bonds in the neighborhood of the proton location.<sup>18,19,25</sup> Empirical valence bond models have been formulated that incorporate the capacity of the proton to undergo a Grothuss-like hopping to a neighboring water molecule.<sup>26–30</sup> However, the computational effort involved in mixed quantum/classical dynamics of proton migration in water<sup>31,32</sup> makes this approach unsuitable for the concentrated protonic solution present in the nanopores of acidic membranes.<sup>25</sup>

Results of molecular modeling have been reported that give information relating the structure of the membrane with the mechanisms of proton conduction.<sup>18,33–35</sup> Using MD simulation, Cui et al.<sup>36</sup> studied the structure and dynamics of hydrated Nafion with water uptake ranging from 5 to 20 wt %. These

\*Corresponding author. Fax: 34-91-5644853. E-mail: riande@ictp.csic.es.

authors found that at 5% the majority of the hydronium ions are hydrated by no more than two molecules of water, prohibiting structural diffusion. As water content increases, the hydronium ion becomes increasingly hydrated and Eigen ions, the necessary step for structural diffusion, are formed. In most cases, full MD simulations of proton transport across cation-exchange membranes and further comparison with experimental results were not performed.<sup>25</sup> However, Ennari et al.<sup>37,38</sup> used MD simulations to calculate the diffusion coefficients of the bare protons, the hydronium ions, and the water molecules in PVF-based polyelectrolytes with different water uptakes. Full molecular dynamics was recently used in our laboratories to simulate separately the diffusion of bare protons and hydrated protons  $\text{H}_3\text{O}^+$  in cation-exchange membranes based on polysulfones, equilibrated with distilled water. A rather good agreement was found between the simulated diffusion coefficient of  $\text{H}_3\text{O}^+$  and that obtained from proton conductivity measurements.<sup>39</sup> Experiments and molecular dynamics were recently combined to investigate the diffusion of water in polyacrylate latex films containing acidic and hydroxyl groups in their structure. Comparing the results forecast with the experimental measurements, it was observed that the mean error was less than 5%.<sup>40</sup>

Pulsed field gradient (PFG) NMR techniques have been widely used to study molecular diffusion of fluids in confined and nonconfined geometries.<sup>41,42</sup> The technique has also been extended to determine apparent diffusion coefficients in acidic ion-exchange membranes with different water contents.<sup>43–46</sup> A study on the diffusion of protons as a function of the water content in Nafion membranes, using independently PFG NMR and impedance spectroscopy, shows that the values obtained for the proton diffusion coefficient by the two techniques are in rather good agreement in the case that the humidity of the membranes is low.<sup>43</sup> However, for membranes with moderate and high water content the difference between the values obtained by the two techniques diverges, the diffusion coefficient of protons obtained from the proton conductivity being higher than that estimated from PFG NMR spin echo experiments.

Owing to the hydrolytic degradation that sulfonated phthalic polyimides present, only hydrolytically stable naphthalenic polyimides are being considered as polyelectrolytes for fuel cells.<sup>47,48</sup> The presence of bulky moieties in the polyelectrolyte chains prevents regular close parallel packing of planar segments that presumably enhance conductivity in low humidity conditions.<sup>49,50</sup> Recently, the synthesis and study of the electrochemical characteristics of sulfonated membranes based on naphthalenic copolyimides, have been reported.<sup>51</sup> In general, the sulfonated naphthalenic copolyimide membranes equilibrated with water exhibit at room temperature conductivities of the same order as those reported for Nafion membranes. Pursuing our research on acidic polyimide membranes, we focus this work on the study of protons diffusion in a representative sulfonated copolyimide membrane, under different humidity conditions, using the PFG NMR spin echo technique. It is the purpose of this work to find out how the proton diffusion coefficients thus obtained,  $D(\text{H}^+)$ , compare with those of both water and the protons intervening in the conductive process. The movement of the bare protons, hydronium ions and water in the membrane containing different humidity will be followed by MD simulation techniques. From the results obtained by NMR, osmotic flow and proton conductivity we shall be able to assess the reliability of full MD simulations to predict the protons diffusivity in sulfonated copolyimides as a function of the degree of humidity.

## Experimental Part

**A. Synthesis and Characterization of a Copolyimide Ion-Exchange Membrane.** A copolyimide material was prepared by

polycondensation of 4,4'-diaminodiphenyl ether (ODA) and 4,4'-diaminodiphenyl ether-2,2'-disulfonic acid (ODADS) with 1,4,5,8-naphthalenetetracarboxylic dianhydride (NTDA). In short, the polymerization was carried out in *m*-cresol, at 180 °C, by one-pot random copolymerization of sulfonated and nonsulfonated diamines, using  $\text{Et}_3\text{N}$  and benzoic acid as the base and catalyst, respectively.<sup>51</sup> The membranes were cast from DMSO solutions (~5 wt %) of the polyelectrolytes onto glass dishes and dried at 80 °C for 10 h. Traces of solvent in the membranes were extracted with methanol at 60 °C for 1 h. The acronym of the membrane is NTDA–ODADS/ODA (3/1) where the ratio between brackets indicates the moles of sulfonated diamine per mole of unsulfonated one utilized in the polymerization process. Chains cross-linking was performed according to a previously reported method in which the dry membranes were immersed into polyphosphoric acid (phosphorus pentoxide content: 86%) at 180 °C for 10 h.<sup>16</sup> The cross-linking was based on phosphorus pentoxide-catalyzed condensation reaction between the sulfonic acid groups of the ODADS moiety and the activated benzene rings of the ODA moiety which yielded the very stable sulfonyl linkages. Then the membranes were thoroughly washed with deionized water and finally dried in vacuum at 120 °C for 10 h.

A schematic representation of the chemical structure of the membrane used in this study is shown in Figure 1. The density of the membranes at room temperature was 1.42 g cm<sup>-3</sup>.<sup>51</sup> The saturated water uptake and ion-exchange capacity of the membranes was 0.874 g and 1.87 mequiv, respectively, referred to 1 g of dry membrane. In the less favorable cases, the error involved in the estimation of the water content was ca. 4%. The proton conductivity of the membrane equilibrated with water was estimated from Bode diagrams calculated using impedance spectroscopic results. The value obtained for this quantity was 8.6 S m<sup>-1</sup> at 25 °C.<sup>51</sup>

**B. NMR Measurements.** The NMR experiments were carried out in a Bruker Avance 400 spectrometer equipped with a 89 mm wide bore, 9.4 T superconducting magnet (proton Larmor frequency at 400.13 MHz).

To determine the diffusion coefficients of water in the acidic copolyimide membrane, the samples were initially hydrated overnight by immersion in distilled water, blotted to remove droplets and transferred to a 5 mm o.d. NMR tube and closed with a plastic cap and wrapped with paraffin film. In successive steps, water in the membrane was partly evaporated in a controlled atmosphere until the reported concentration was reached. Owing to very rapid evaporation processes taking place in the fully hydrated membranes, the NMR experiments were restricted to membranes with water content lying in the range  $0 < w < 0.65$ . In all cases, the proton NMR measurements were performed after allowing 48 h for equilibration of moisture within the tube volume. Samples were weighted with a precision of 0.1 mg before and after measurements and no significant weight loss was observed (< 1%).

The proton diffusion reported data were acquired at  $25 \pm 1$  °C with a Bruker diffusion probehead Diff60 using 90°  $^1\text{H}$  pulse lengths between 6.0 and 6.5  $\mu\text{s}$ . An inversion–recovery pulse sequence was used to estimate the longitudinal relaxation times,  $T_1$ , of absorbed water protons. A pulsed field gradient stimulated spin echo pulse sequence was used. The echo time between the first two 90° rf pulses,  $\tau_1$ , varied between 2.71 and 3.11 ms. The apparent diffusion coefficient of protons,  $D$ , was measured at diffusion times,  $\Delta$ , of 10 and 20 ms, varying the length of the gradient pulses between 1.6 and 2.0 ms, and their amplitude between 0 and 14 T m<sup>-1</sup>. The repetition rate was 3 s. The total acquisition time for these experiments varied from 20 min to 6 h. The decay of the echo amplitude was monitored typically to > 30% of its initial value and the apparent diffusion coefficient at a given  $\Delta$  was calculated by fitting a stretched exponential function to the decay curve. All proton spectra were externally referenced to an aqueous solution of DSS

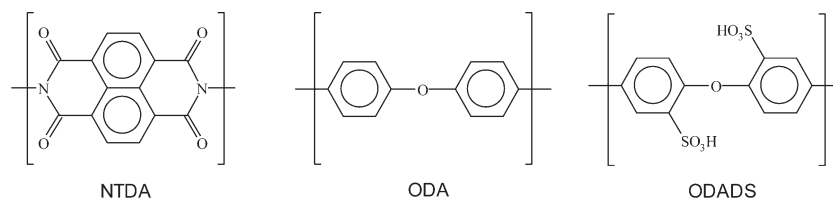


**Figure 1.** Schematic representation of monomer units included in the PEI membranes studied.

**Table 1.** Description of the Different Simulated Cells

chains	number of particles				$L_X = L_Y = L_Z, \text{\AA}$	mol of $\text{H}_2\text{O}$ /equiv of $\text{SO}_3^-$	g of $\text{H}_2\text{O}$ /g of dry membrane
	$\text{H}^+$	$\text{H}_2\text{O}$	$\text{H}_3\text{O}^+$	$\text{H}_2\text{O}$			
3	24	24	24	0	25.04	1	0.034
3	24	96	24	72	26.15	4	0.135
3	24	120	24	96	26.47	5	0.169
3	24	168	24	144	27.05	7	0.236
3	24	240	24	216	28.15	10	0.337
3	24	288	24	264	28.58	12	0.405
3	24	360	24	336	29.60	15	0.506
3	24	408	24	384	30.10	17	0.573
3	24	480	24	456	30.91	20	0.674
3	24	622	24	598	32.27	25.9	0.870

(sodium 4,4-dimethyl-4-silapentane-1-sulfonate). Previously, the gradient was calibrated according to the spectrometer manufacturer protocol, using a sample of water doped with  $\text{CuSO}_4$  at  $1.0 \text{ g L}^{-1}$  and a value of the water diffusion coefficient equal to  $2.3 \times 10^{-9} \text{ m}^2 \text{ s}^{-1}$ . Furthermore, the calibration was verified at the range of gradient values used experimentally by measuring the diffusion coefficient of dry glycerol. It was found to have a value of  $D = 2.23 \times 10^{-12} \text{ m}^2 \text{ s}^{-1}$ , in good agreement with those reported in the literature.<sup>52</sup>

**C. Computational Details of Molecular Dynamics.** Bulk structures of NTDA-ODADS/ODA (3/1) (see Figure 1) of molecular weight 4269.72 g/mol with sulfonic acid anions ( $-\text{SO}_3^-$ ) anchored to the matrix, and water absorbed, were generated and simulated by means of the Accelrys commercial software (Materials Studio 3.2, Accelrys Inc., San Diego, CA)<sup>53</sup> using the PCFF91 force field.<sup>54</sup> The number of fixed ionic groups in the bulk structures was set equal to the IEC of the membrane, 1.87 mequiv/(g of dry polyelectrolyte). All the MD simulations were performed under NVT conditions with the working temperature of 298 K controlled by means of the Andersen thermostat method with a collision ratio of 1.0. The density of the systems was calculated by weight fraction of polymer–water with densities of  $1.42 \text{ g cm}^{-3}$  and  $1 \text{ g cm}^{-3}$  for polymer system and water respectively; the volume of each system was the same regardless of the working temperature. For the integration of the atomic motion equations, a time step  $\delta = 1 \text{ fs}$  (i.e.,  $10^{-15} \text{ s}$ ) was used. The van der Waals and Coulombic nonbonding interactions were calculated by the cell multipole method (CMM).<sup>55</sup> The value of the update width parameter was 1.0 Å, and the accuracy parameter was set to medium to use third order in the Taylor series expansion and explicit interactions form more neighboring cells.<sup>56</sup> The structural results obtained by using the fast CMM methods for the cells agree with the results obtained with the slow Ewald summation method.<sup>57</sup> Membranes consisting on 3D amorphous cells with periodic boundary conditions and containing different amounts of polymer, water and diffusion particles were built using the Amorphous\_cell module of the software. Each cell contained tree chains of NTDA–ODADS/ODA (3/1) (see Figure 1), with IEC of 1.87 mequiv/(gram dry membrane)<sup>51</sup> and different amounts of  $\text{H}^+$ ,  $\text{H}_3\text{O}^+$ , and  $\text{H}_2\text{O}$ . The lengths of the cubic structures and the composition of the system contained in each cell are summarized in Table 1.

The PCFF force field<sup>54,58–60</sup> was found to be suitable for modeling water swollen polyelectrolyte systems.<sup>44</sup> For example,

this software was used by Grujicic et al.<sup>61</sup> for MD simulations of the conductivity of polyelectrolytes and by Chen et al.<sup>62</sup> to simulate the diffusion of water in polyacrylate films. Charges were calculated by the QEq charged 1.1 module<sup>63</sup> which is available in Materials Studio software. The structure of each system was first minimized with respect to all the internal coordinates by a Conjugate Gradient method until the maximum derivative was smaller than  $0.1 \text{ kcal}/(\text{\AA} \text{ mol})$ , with a limit of 5,000 steps. Then, the system was submitted to an equilibration process consisting on a 200 ps ( $2 \times 10^{-10} \text{ s}$ ) long MD run. The data collecting stage consisted on MD runs of 3 ns ( $3 \times 10^{-9} \text{ s}$ ) for all systems. In both cases, the trajectories were saved each 500 fs for subsequent analysis. A visual scheme of the fully hydrated MD cell is shown in Figure 2. As occurs with semiflexible polyelectrolytes, like Nafion, segregation of hydrophilic domains from the hydrophobic ones takes place appearing channels bordered with  $-\text{SO}_3^-$  groups attached to the polyimide matrix surrounded of molecules of water and protons.

## Results

**A. PFG NMR.** PFG NMR methods to measure diffusion of protons in cation-exchange membranes are based on the relationship between the resonance frequency of the nucleus of interest and the external magnetic field it experiences, as expressed by the Larmor equation:  $\omega_0 = -\gamma B_0$ . The application of a magnetic field gradient across the sample volume labels magnetically molecules having NMR sensitive nuclei enabling the tracking of their motion over a given time, the diffusion time. In practice, this is accomplished using a spin echo type of pulse sequence, as first described by Stejskal et al.<sup>64</sup> The application of three consecutive and suitably spaced  $\pi/2$  radiofrequency (rf) pulses generates an observable NMR signal (echo) centered at a time equal to  $2\tau_1 + \tau_2$  from the first rf pulse, where  $\tau_1$  is the time separation between the first two rf pulses and  $\tau_2$  is the time elapsed between the second and the third rf pulses. The magnetic labeling is accomplished by applying two gradient pulses of amplitude and duration  $g$  and  $\delta$ , respectively, spaced by a time  $\Delta$ , the diffusion time. In the absence of motion, the loss of phase coherence of the NMR signal caused by the first gradient pulsed would be compensated by the second gradient pulse, but this would not be the case



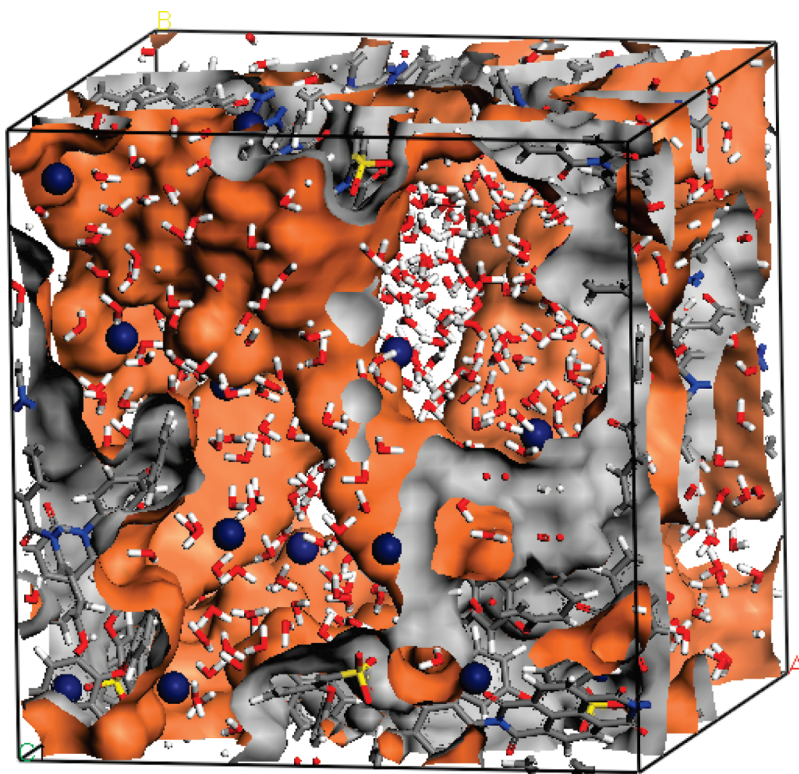


**Figure 2.** Visual scheme of the fully hydrated MD cell with isosurfaces of polymer chains. Box size: 32.27 Å. Atoms (color): O (red), C (gray), H (white), S (yellow), N (blue), and  $\text{H}^+$  or  $\text{H}_3\text{O}^+$  (blue spheres).

if molecular diffusion occurs during the time  $\Delta$ . Then, an attenuation of the echo is observed as expressed by

$$A(g) = A(0) \exp(-bD) \quad (1)$$

where  $A(g)$  and  $A(0)$  are the amplitude of the echo in the presence of a gradient pulse with amplitude  $g$  and  $\theta$ , respectively,  $b = (\gamma g \delta)^2 (\Delta - \delta/3)$  where  $\gamma$  is the gyromagnetic ratio of the nucleus being observed, and  $D$  is the diffusion coefficient. Knowing  $D$  and considering that the mean square displacement in one direction is given by

$$\langle x \rangle^2 = 2D\Delta \quad (2)$$

the PFG NMR measurements allow probing the membrane morphology at molecular level and its effect upon transport properties.

Prior to performing the diffusion measurements, the proton signal corresponding to water absorbed in the membranes was analyzed. At high degree of hydration, above 0.40 g of  $\text{H}_2\text{O}/(\text{g}$  of dry membrane), the proton spectra are dominated by a signal at 4.8–4.9 ppm with a line width of 160–180 Hz and a spin–lattice relaxation time,  $T_1$ , of about 40 ms (see Figure 3). Minor proton signals are observed at lower field, up to 13 ppm. In addition, three peaks at 2.4, 1.1, and 0.7 ppm are observed with slightly longer  $T_1$ s,  $\sim 90$  ms. The various types of resonances present in hydrated membranes are more visible in a proton diffusion-weighted spectrum ( $g = 350 \text{ G cm}^{-1}$ ) as illustrated in Figure 4. Here, the peak intensity is attenuated as a function of the corresponding value of its diffusion coefficient. The protons with the largest diffusion coefficient (i.e., at 4.9 ppm) appear strongly attenuated and enable the visibility of those protons with smaller diffusion coefficients (i.e., those in the region between 2.4 and 0.7 ppm).

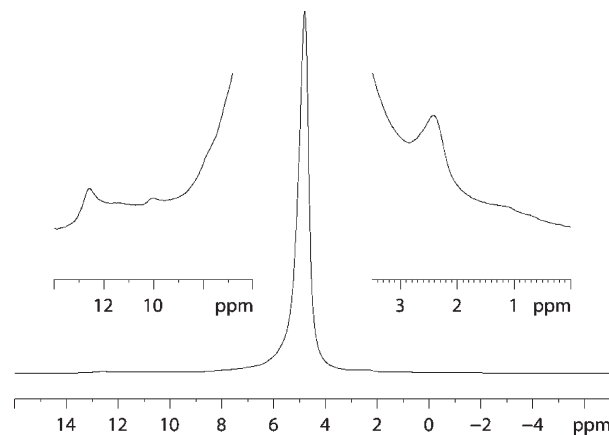


**Figure 3.** Proton NMR spectrum corresponding to a sulfonated PEI membrane with 0.65 g of  $\text{H}_2\text{O}/(\text{g}$  of dry membrane) water content. The insets illustrate the presence of protons in the high and low field spectral regions.

At lower degrees of hydration, less than 0.26 g of  $\text{H}_2\text{O}/(\text{g}$  of dry membrane), the main peak shifts to lower fields (5.3–5.7 ppm), the line width increases (250–500 Hz) and  $T_1$  decreases ( $\sim 24$  ms). As the water content decreases, the observed changes could be attributed to alterations in the distribution of water molecules in the polymer matrix and interactions water–polymer chains. The peak at 2.4 ppm is visible at water concentrations above 0.40 g of  $\text{H}_2\text{O}/(\text{g}$  of dry membrane). The peaks at higher field, 1.1 and 0.7 ppm, remain visible even after drying the membranes during 48 h at 130–140 °C under vacuum, and exhibit an increase in the value of  $T_1$  to 360 ms.

Since the PFG methods are based on the observation of an echo, the rapid decay of the proton signal (short spin–spin

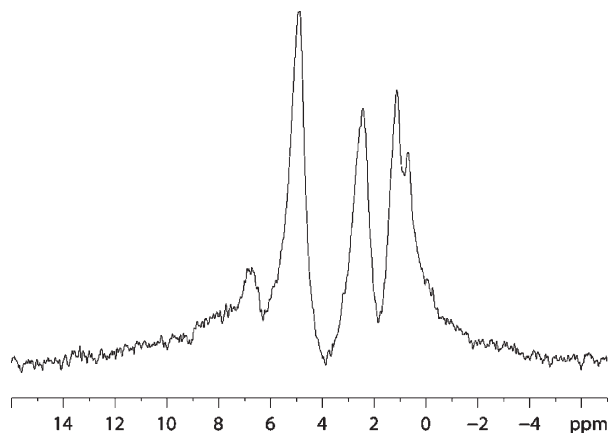


**Figure 4.** Diffusion-weighted proton spectrum corresponding to a sulfonated PEI membrane with water content of 0.50 g of H<sub>2</sub>O/(g of dry membrane). The duration and amplitude of the applied pulsed field gradients were 2 ms and 350 G cm<sup>-1</sup>, respectively.

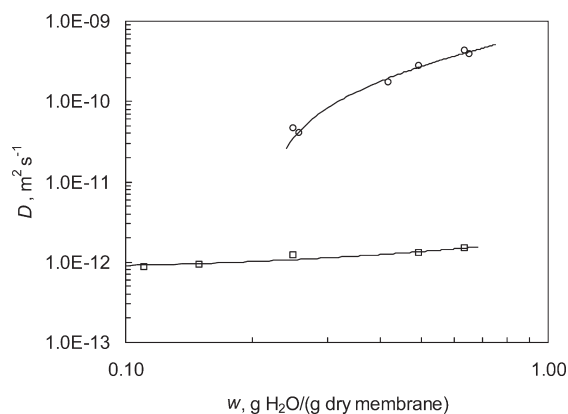


**Figure 5.** Variation of water–proton diffusion coefficients for sulfonated PEI membranes in acidic form with the degree of hydration. The circles and squares correspond to the measurements for peaks at 5 and 1 ppm, respectively.

relaxation time,  $T_2$ ) leads to a significant reduction in the signal-to-noise ratio of the spectrum, thus limiting the practical range of some experimental parameters, i.e., diffusion times, and requiring an increase in signal averaging to improve detection. Here, a stimulated spin echo sequence was chosen because it allows short echo times and the diffusion time is limited by  $T_1$ .

Taking into account that a continuum spectrum of diffusion coefficients might be a more realistic description of the systems under consideration than that provided by a set of discrete values (i.e., multiexponential fit), the data were fitted to a fractional exponential function

$$A(g) = A(0) \exp[-(bD_{app})^\beta] \quad (3)$$

where  $\beta$  is a “stretch” coefficient lying in the range  $0 < \beta \leq 1$ ,  $D_{app}$  is the apparent diffusion coefficient and the rest of the variables as previously described. Although we observed several peaks in the proton spectra of hydrated membranes, the overwhelming water signal about 5 ppm and the similarity of apparent diffusion values of the protons associated to smaller peaks allowed only the unambiguous characterization of the diffusion coefficients associated to the resonances at about 5 and 1 ppm. The results are collected in Table 2. As shown in Figure 5, the values of  $D_{app}$  for water protons (4.8–5.3 ppm) decrease nonlinearly and by an order of magnitude

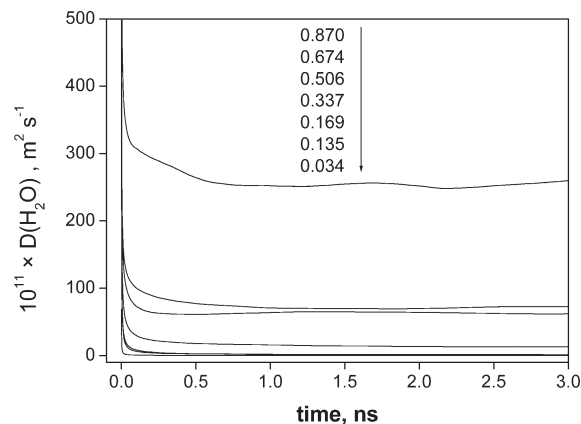


**Figure 6.** Dependence of the diffusion coefficient of water on time for membranes with different water content that decreases from top to bottom, as indicated in the inset.

as the degree of hydration decreases from 0.65 to 0.25 g of H<sub>2</sub>O/(g of dry membrane), while the value of  $\beta$  remains constant, about 1 in all cases. This suggests a relatively uniform environment for this type of protons, at least in the time scales studied. Diffusion measurements at longer diffusion times are hampered by the short relaxation times of the absorbed water protons, as indicated above.

The protons at 1.1–0.7 ppm exhibit diffusion coefficients nearly 2 orders of magnitude smaller than those of bulk water in the membrane. As shown in Figure 5, the diffusion coefficient of the residual water exhibits a slight increasing linear dependence on the degree of hydration over the entire range studied. The values of  $\beta$  are somewhat smaller than for bulk water, they are about 1.0–0.7 and suggest a more heterogeneous environment for these protons, not averaged during the time course of the measurement.

**B. Full MD Simulations.** Diffusion coefficients in cation-exchange membranes can be calculated by the Einstein diffusion equation<sup>65</sup>

$$D = \frac{1}{6N} \lim_{t \rightarrow \infty} \frac{d}{dt} \sum_{i=1}^N \langle [\mathbf{R}(t) - \mathbf{R}(0)]^2 \rangle \quad (4)$$

The sum term on the right-hand side of the equation over  $N$  is called the mean square displacement (MSD).  $N$  is the number of diffusing molecules,  $t$  is time and  $\mathbf{R}(t)$  is the position vector of a molecule at time event  $t$ . Average MSD curves as a function of time for each diffuser type were calculated. In general, the values of  $D$  decrease as time increases, reaching a constant value at long times that reflect particles diffusion in steady state conditions ( $t \rightarrow \infty$ ). In this situation,  $\Delta[\log(\text{MSD})]/\Delta[\log t] = 1$ . Illustrative plots showing this behavior for the diffusion coefficient of water for membranes with different water content are shown in Figure 6. Values of the diffusion coefficient of protons, hydronium ions and water computed from the corresponding trajectories by means of eq 4 are shown as a function of the water content  $w$  in Figure 7. In general  $D(\text{H}^+) > D(\text{H}_3\text{O}^+) > D(\text{H}_2\text{O})$ . As expected, both the diffusion coefficients and the difference between the diffusion coefficients of the particles for a given  $w$  increase as  $w$  increases. Thus for low values of  $w$  lying in the range  $0.034 \leq w \leq 0.169$ , where  $w$  is given in g of H<sub>2</sub>O/(g of dry membrane), the results for the diffusion coefficients expressed in terms of  $10^{11} \times D$  in m<sup>2</sup> s<sup>-1</sup> units vary from 0.08, 0.20, and 0.52 for H<sup>+</sup>, H<sub>3</sub>O<sup>+</sup> and H<sub>2</sub>O, respectively, to 1.44, 0.97 and 4.51, respectively. For  $w > 0.169$  g of H<sub>2</sub>O/(g of dry membrane) the diffusion coefficients undergo

a sharp increase with the water content, especially the diffusion coefficient of the bare protons which reaches a value of  $2.76 \times 10^{-9} \text{ m}^2 \text{ s}^{-1}$  for  $w = 0.674$ , roughly three times the value of the diffusion coefficient computed for  $\text{H}_3\text{O}^+$ . Finally the value simulated for the diffusion coefficient of water is  $1.12 \times 10^{-9} \text{ m}^2 \text{ s}^{-1}$  in the membrane containing 0.674 g of  $\text{H}_2\text{O}/(\text{g of dry membrane})$ , a value slightly lower than that found for  $\text{H}^+$  with the same water content.

The distribution of the molecules of water in the conformational landscape of the polyelectrolyte was investigated by computing intermolecular pair correlations functions  $g_{AB}(r)$ , which represent the probability of finding a pair of

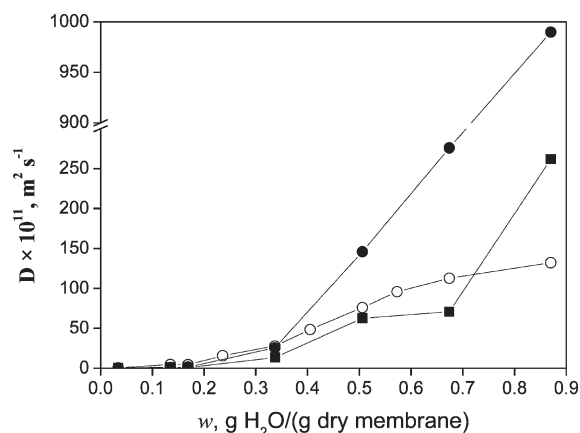


**Figure 7.** Dependence of the diffusion coefficient obtained by MD simulations on the water content of the membranes for bare protons (filled circles), hydronium ions (filled squares), and water (open circles).

**Table 2.** Diffusion Coefficients of Water Protons in Sulfonated PEI Membranes Measured with PFG NMR at 25 °C

$\delta$ (ppm)	$w$ , g of $\text{H}_2\text{O}/$ (g of dry membrane)	$10^{11} \times D_{app}$ , $\text{m}^2 \text{ s}^{-1}$ <sup>a</sup>	$\beta$ <sup>a</sup>
4.80	0.650	39.2 (0.05)	1.00 (0.02)
4.80	0.633	43.0 (0.04)	1.00 (0.03)
4.92	0.496	27.9 (0.04)	0.98 (0.02)
4.82	0.420	17.1 (0.02)	1.04 (0.03)
5.30	0.257	4.01 (0.05)	0.95 (0.02)
5.34	0.250	4.71 (0.05)	0.98 (0.02)
2.41	0.633	2.5 (0.2)	0.71 (0.03)
2.47	0.496	0.67 (0.04)	0.74 (0.05)
1.09	0.633	0.15 (0.02)	0.8 (0.2)
1.14	0.496	0.13 (0.02)	0.8 (0.2)
1.12	0.250	0.12 (0.01)	0.7 (0.2)
1.15	0.150	0.094 (0.009)	1.0 (0.1)
1.14	0.111	0.086 (0.009)	0.79 (0.08)
1.28	residual water	0.078 (0.009)	0.71 (0.08)

<sup>a</sup> Standard deviation in parentheses

**Table 3.** Coordination Numbers of Fixed Anionic Groups and Mobile Particles, First Coordination Shell in Å and  $\langle n(1) \rangle$

g of $\text{H}_2\text{O}/\text{g of dry membrane}$	0.034	0.135	0.169	0.337	0.506	0.674
mol of $\text{H}_2\text{O}/\text{equiv of SO}_3\text{H}$	1	4	5	10	15	20
$x \cdots z$						
$\text{O}_3\text{S} \cdots \text{H}^+$	2.85 (1.12)	2.95 (0.96)	3.05 (0.80)	3.05 (0.79)	3.45 (0.85)	3.45 (0.76)
$\text{O}_3\text{S} \cdots \text{OH}_2^a$	4.05 (1.38)	4.25 (4.81)	4.25 (7.92)	4.25 (6.72)	4.35 (8.34)	4.35 (9.30)
$\text{H}^+ \cdots \text{OH}_2$	2.15 (0.76)	2.35 (2.04)	2.35 (2.61)	2.45 (3.38)	2.55 (3.94)	2.65 (4.60)
$\text{O}_3\text{S} \cdots \text{OH}_3^+$	3.15 (0.71)	3.45 (1.21)	3.55 (1.74)	3.55 (1.57)	3.65 (1.76)	3.65 (1.65)
$\text{O}_3\text{S} \cdots \text{OH}_2^b$		4.15 (2.99)	4.15 (3.88)	4.15 (5.32)	4.15 (7.01)	4.25 (8.00)
$\text{H}_3\text{O}^+ \cdots \text{OH}_2$		2.95 (2.09)	2.95 (2.52)	2.95 (3.52)	3.05 (4.02)	3.05 (4.79)
N in imide $\cdots \text{OH}_2$	4.45 (2.18)	4.95 (3.54)	4.95 (5.17)	4.95 (6.88)	4.95 (7.35)	4.95 (7.52)

<sup>a</sup> Molecular dynamics simulation with bare-protons,  $\text{H}^+$  <sup>b</sup> Molecular dynamics simulation with hydrated-protons,  $\text{H}_3\text{O}^+$

particles AB at a distance  $r \pm dr$  normalized with respect to the probability expected for a completely random distribution at the same density. Values of  $g_{AB}(r)$  were evaluated as<sup>53</sup>

$$g_{AB}(r) = \frac{V \langle \sum_{i \neq j} \delta(r - |\mathbf{r}_{Ai} - \mathbf{r}_{Bj}|) \rangle}{(N_A N_B - N_{AB}) 4\pi r^2 dr} \quad (5)$$

where A and B represent two kinds of particles (e.g., individual atoms, ions such as  $\text{H}^+$ , atomic groups like  $\text{H}_3\text{O}^+$ , etc.). The system has a volume  $V$  and contains  $N_A$  particles of kind A and  $N_B$  particles of kind B with  $N_{AB}$  particles belonging simultaneously to both kinds ( $N_A = N_B = N_{AB}$  when computing correlation among particles of the same kind; for instance, correlation of the relative positions of  $\text{H}^+$  ions). Vectors  $\mathbf{r}_{Ai}$  and  $\mathbf{r}_{Bj}$  represent the position of particle  $i$  of kind A and particle  $j$  of kind B, so that  $|\mathbf{r}_{Ai} - \mathbf{r}_{Bj}|$  is the distance between those two particles. The term  $\delta(r - |\mathbf{r}_{Ai} - \mathbf{r}_{Bj}|)$  is set to unity when  $(r - |\mathbf{r}_{Ai} - \mathbf{r}_{Bj}|) \leq dr$  (i.e., when the difference between desired and actual distance among the two particles is smaller than a tolerance factor  $dr$ ) and to zero otherwise.

Values of  $g(r)$  can be converted into coordination numbers by means of the following expression:

$$n_{x \cdots z}(r) = 4\pi \frac{N_z}{\langle V \rangle} \int_0^r g_{x \cdots z}(s) s^2 ds \quad (6)$$

where  $n_{x \cdots z}(r)$  is the number of  $x$  particles coordinated to particle  $z$  within a radius  $r$ ,  $\langle V \rangle$ , the cell volume,  $N_z$ , the total number of particles  $z$  in the system and  $g_{x \cdots z}(s)$ , the radial distribution function between  $x$  and  $z$ . The size of the coordination shells are collected in Table 3. In the same table, between brackets, the computed results for coordination numbers involving fixed anionic groups and mobile particles in first coordination shells are shown. An inspection of the results shows that the size of the coordination shells slightly increases with the water content. The coordination number reflecting the number of  $\text{H}^+$  particles around the sulfonate anion is nearly independent of the water content of the membrane, lying in the vicinity of the unit. On the other hand, the values of the coordination number for  $\text{H}_3\text{O}^+$  around  $-\text{SO}_3^-$  lie below 2. It is 0.71 and 1.21 for the membranes with  $w = 0.034$  and 0.135 g of  $\text{H}_2\text{O}/(\text{g of dry membrane})$ , respectively, increasing up to roughly 1.7 for membranes with higher water content. It is worth noting that the number of molecules of water in the shell around  $-\text{SO}_3^-$  undergoes a significant augment with increasing water content, from 1.38 for  $w = 0.034$  g of  $\text{H}_2\text{O}/(\text{g of dry membrane})$  to 9.30 for  $w = 0.674$  in the same units. Also the coordination numbers for  $\text{H}_3\text{O}^+ \cdots \text{O}$  in  $\text{H}_2\text{O}$  and  $\text{H}^+ \cdots \text{O}$  in  $\text{H}_2\text{O}$  increase with increasing water content of the membranes, though the increase is lower than that found for the



coordination number of S in  $\text{O}_3\text{S}\cdots\text{O}$  in  $\text{H}_2\text{O}$ . Finally, the number of molecules of water surrounding the imide groups is in most cases slightly lower than those surrounding the  $-\text{SO}_3^-$  anions.

For reasons that will be outlined below, the trajectories of the imide groups were followed as a function of time for membranes with different water contents finding that the diffusion coefficient of the moieties lies in the vicinity of  $11.3 \times 10^{-13} \text{ m}^2 \text{ s}^{-1}$  for membranes with low water content. For high water content, the diffusion coefficient does not follow a definite trend, the lower and upper bounds of the values of this parameter being  $30.9 \times 10^{-13} \text{ m}^2 \text{ s}^{-1}$  and  $96.3 \times 10^{-13} \text{ m}^2 \text{ s}^{-1}$ , respectively.

## Discussion

The proton NMR spectra of hydrated membranes show peaks at chemical shifts spanning from 1 to 14 ppm. The peaks between 4 and 13 ppm are attributed to acidic protons in various environments, and water protons.<sup>46,66</sup> Resonances at higher fields, between 1.0 and 1.3 ppm, have been attributed to hydration water in membranes of hexafluorinated sulfonated poly(arylene thioether sulfone) copolymers.<sup>67</sup> On the other hand, small peaks between 1 and 3 ppm have been observed in the proton spectra of perfluorosulfonate ionomer membranes and attributed to residues of alcohols used in the solvent mixture for films casting.<sup>46</sup> After considering the various solvents and nonsolvents used in the preparation of the membranes subject of study here, we attribute the resonances appearing in this region to water protons. These protons are difficult to remove under experimental conditions that do not compromise the chemistry and physical integrity of the membranes. In fact, the peaks at 0.7–1.1 ppm are still observed after heating the samples during two days at  $\sim 130^\circ\text{C}$  in vacuum. We checked this hypothesis by performing NMR experiments on a solvent cast nonsulfonated poly(ether imide) membrane. After being hydrated 24 h in distilled water, the corresponding proton spectrum exhibited three resonances at 1.94, 4.58, and 6.34 ppm. Upon drying the membrane under more extreme conditions (four days near  $200^\circ\text{C}$  in vacuum), its proton spectrum showed only noise. It has been reported that polyimides with chemical structures similar to those used in this study have 0.05–0.10 g of “residual” water/(g of dry membrane) that it is not easily removed.<sup>68</sup> In addition, studies of water absorbed in polyimide films have shown that water molecules aggregate near carbonyl groups of the imide rings.<sup>69</sup> Thus, we attribute the presence of these peaks to water associated with the polymer in cavities formed primarily by chain segments with highly delocalized electron density since this water proton resonance appears shifted to low fields by about 4 ppm. To check this assumption we simulated the diffusion coefficient of the imide group finding that the value of this parameter is of the same order of magnitude as that of the water located in this region for membranes with low water content. In this case, it happens as whether molecules of water were physically bound to the electrophilic moiety involving the bicarbonyl–imide group. However, for membranes with high water content the simulations overestimate the values of  $D(^1\text{H})$  obtained for water centered at 1 ppm.

After describing the determination of the diffusion coefficient it is convenient to discuss what it means. In acidic ion exchange membranes equilibrated with water,  $^1\text{H}$  nuclei exchanges rapidly between water and  $\text{H}^+$  where this later ionic specie covers all forms, including aqueous complexes, of  $\text{H}^+$  in different environments of the hydrated acidic membrane. As a result, the diffusion coefficient of  $^1\text{H}$  is the weighted average of the diffusion coefficients for the separate environments. This consideration suggests that the diffusion coefficient measured by spin echo in this work may not exactly be the self-diffu-

sion coefficient of water in the membrane. One would expect that in membranes with high water uptake the  $^1\text{H}$  diffusion coefficient  $D(^1\text{H})$  would identify with that of water since in this case the concentration of  $^1\text{H}$  of water would be much larger than that of  $\text{H}^+$ .

Recent experimental work carried out on the NTDA–ODADS/ODA (3/1) membrane saturated with water ( $w = 0.874 \text{ g of H}_2\text{O}/(\text{g of dry membrane})$ )<sup>51</sup> shows that the diffusion coefficient of water  $D(\text{H}_2\text{O})$  determined from osmotic flow is  $1.91 \times 10^{-9} \text{ m}^2 \text{ s}^{-1}$ , a value close to the self-diffusion coefficient reported for water at  $25^\circ\text{C}$  which amounts to  $2.2 \times 10^{-9} \text{ m}^2 \text{ s}^{-1}$ .<sup>70</sup> However, owing to anomalous osmotic flow the value of  $D(\text{H}_2\text{O})$  obtained from osmotic flow may be overestimated. Actually, the osmotic measurements were carried out using the configuration distilled water/NTDA–ODADS/ODA (3/1) membrane/low concentration HCl solution. Protons in the solution migrate to the side of the membrane in contact with the water compartment creating a potential that drives the charged pore liquid to the solution compartment. In other words, osmotic flow occurs under the combined action of an electric field and a chemical field, that is, an electrochemical field.<sup>51</sup> The effect of the field on the osmotic flow is made evident if a diluted sodium chloride solution replaces the low concentration HCl solution in the configuration indicated above. In this case the value of  $D(\text{H}_2\text{O})$  obtained from the osmotic flow decreases to  $7.4 \times 10^{-10} \text{ m}^2 \text{ s}^{-1}$ .<sup>51</sup> Taking into account that the maximum water content of the membrane used in the NMR experiments was 0.650 g of  $\text{H}_2\text{O}/(\text{g of dry membrane})$  whereas the saturated water uptake in the osmotic measurements was 0.874 in the same units, the results obtained for  $D(\text{H}_2\text{O})$  from osmotic measurements are in reasonable agreement with  $D(^1\text{H})$  obtained from spin echo NMR measurements.

Results for MD simulations of the diffusion coefficients of bare protons and hydronium ions are shown as a function of the water content of the membrane in Figure 7. As expected, the diffusion coefficient of protons is higher than that of hydronium ions, whatever the water content of the membrane is. The difference between  $D(\text{H}^+)$  and  $D(\text{H}_3\text{O}^+)$  increases as  $w$  increases. Usually the value of the diffusion coefficient intervening in the conductivity is obtained from the Nernst–Planck equation as

$$D(\text{H}^+) = \frac{\sigma RT}{c(\text{H}^+)F^2} \quad (7)$$

where  $\sigma$  and  $F$  are, respectively, the proton conductivity and Faraday’s constant,  $c(\text{H}^+)$  is the concentration of protons in the membrane and  $RT$  is the thermal energy. Zawodzinski et al.<sup>43</sup> carried out a thorough study on the water content dependence of both the diffusion coefficient of protons  $D(^1\text{H})$  obtained by PFG NMR and the diffusion coefficients of protons  $D(\text{H}^+)$  estimated from conductivity measurements in Nafion membranes. For membranes with low water content the values of  $D(^1\text{H})$  and  $D(\text{H}^+)$  are rather similar, suggesting that the mechanism involved in proton transport is of vehicular type. For moderate and high water content  $D(\text{H}^+) > D(^1\text{H})$ , and the difference between them,  $D(\text{H}^+) - D(^1\text{H})$ , increases as the water content increases. Under these circumstances, proton transport in the membranes is of the structural type. An inspection of the results of Figure 7 shows a similar behavior for the NTDA–ODADS/ODA (3/1) membrane. Actually, the simulated values of the diffusion coefficients of bare protons  $D(\text{H}^+)$ , hydronium ions  $D(\text{H}_3\text{O}^+)$  and the experimental NMR result  $D(^1\text{H})$  in membranes with  $w \leq 0.20 \text{ g of H}_2\text{O}/(\text{g of dry membrane})$  are similar. However, for higher water contents,  $D(\text{H}^+) > D(\text{H}_3\text{O}^+) > D(^1\text{H})$  and the difference between the diffusion coefficients increases as the water content increases. Unfortunately we do not have on hand of data referred

to the variation of the proton conductivity of the NTDA–ODADS/ODA (3/1) membrane with the water content. However, we have measured the conductivity of the membrane equilibrated with water ( $w = 0.837$  g of  $\text{H}_2\text{O}$ /(g of dry membrane)) and the pertinent value of this quantity is  $8.6 \text{ S m}^{-1}$ , at  $25^\circ\text{C}$ . From eq 7 it follows that the experimental value of  $D(\text{H}^+)$  is  $2.2 \times 10^{-9} \text{ m}^2 \text{ s}^{-1}$ .<sup>71</sup> It is remarkable that this result is very close to that obtained by simulation for  $D(\text{H}_3\text{O}^+)$ ,  $2.6 \times 10^{-9} \text{ m}^2 \text{ s}^{-1}$ . However, the value obtained for the diffusion coefficient of bare protons is nearly four times that estimated from the conductivity measurements. Then the simulation of diffusion of the hydronium ion, though a crude resemblance of the structural diffusion of proton in the membrane phase, gives a reasonably good account of the diffusion of protons in the copolyimide membrane. Similar good agreement between the simulated value of  $D(\text{H}_3\text{O}^+)$  and that obtained from conductivity measurements was found for fully hydrated acidic membranes based on polyphenyl ether sulfones.<sup>15</sup>

## Conclusions

<sup>1</sup>H NMR spectra of hydrated naphthalenic imide membranes show peaks at chemical shifts spanning from 1 to 14 ppm. The peaks between 4 and 13 ppm are attributed to acidic protons in various environments and water protons. The main resonance, centered in the vicinity of 5 ppm in the spectra of membranes with high water content, is slightly shifted to higher chemical shifts for membranes with low water content. The resonance peaks centered in the vicinity of 1 ppm are attributed to molecules of water difficult to remove from the membrane, even in conditions that involve the heating of the membrane at  $130$ – $140^\circ\text{C}$  in vacuum. The value of  $D(\text{H}^+)$  for this type of water is about 2 orders of magnitude below that corresponding to the water whose proton resonance peak is centered in the vicinity of 5 ppm. Also  $D(\text{H}^+)$  is of the same order of magnitude as the diffusion coefficient of the imide group for membranes with low water content, as calculated by molecular dynamics simulations. This result suggests that the water associated with the peak at 1 ppm might be physically associated with the hydrophilic imide moiety.

For the fully hydrated membranes, the values of  $D(\text{H}_3\text{O}^+)$  and  $D(\text{H}_2\text{O})$  are in rather good agreement with those obtained for these quantities from the proton conductivity and osmotic flow, respectively. It seems then that simulation of the molecular trajectory of these particles allows predicting their diffusive properties, apparently without the need of using the structural mechanisms of proton transport. However, this approach fails if bare protons are used as diffusing particles in MD simulations.

**Acknowledgment.** This work was supported by Comunidad de Madrid (CAM Project S-0505/MAT/0227) and the CICYT (Projects CTQ2005-04710/BQU, MAT2005-05648-C02-01, and MAT2007-63722).

## References and Notes

- Mauritz, K. A.; Moore, R. B. *Chem. Rev.* **2004**, *104*, 4535.
- Alberti, G.; Casciola, M. *Solid State Ionics* **2001**, *145*, 3.
- Summer, M. J.; Harrison, W. L.; Weyers, R. M.; McGrath, J. E.; Riffle, J. S.; Brink, A.; Brink, M. H. *J. Membr. Sci.* **2004**, *239*, 199.
- Damay, F.; Klein, L. C. *Solid State Ionics* **2003**, *162*–*163*, 261.
- Wang, H.; Holmberg, B. A.; Huang, L.; Wang, Z.; Mitra, A.; Norbeck, J. M.; Yan, Y. *J. Mater. Chem.* **2002**, *12*, 834.
- Mauritz, K. A.; Payne, J. T. *J. Membr. Sci.* **2000**, *168*, 39.
- Navarra, M. A.; Croce, F.; Scrosati, B. *J. Mater. Chem.* **2007**, *17*, 3210.
- Costamagna, P.; Yang, C.; Bocarsli, A. B. *Electrochim. Acta* **2002**, *47*, 1023.
- Hickner, M. A.; Chasse, H.; Kim, Y. S.; Einsla, B. R.; McGrath, J. E. *Chem. Rev.* **2004**, *104*, 4587.
- R&D Plan for the High Temperature Membrane Working Group, U.S. Department of Energy, Office of Efficiency and Renewable Energy's Hydrogen, Fuel Cells & Infrastructure Technology Program, 2003.
- Li, Q. F.; He, R. H.; Jensen, J. O.; Bjerrum, N. J. *Chem. Mater.* **2003**, *15*, 4896.
- Mauritz, K. A.; Moore, R. B. *Chem. Rev.* **2004**, *104*, 4535.
- Jannasch, P. *Curr. Opin. Colloid Interface Sci.* **2003**, *8*, 96.
- Ye, G.; Mills, C. M.; Godward, G. R. *J. Membr. Sci.* **2008**, *319*, 238.
- Parceros, C. E.; Fernández-Carretero, J. F.; Compañ, V.; Herrera, R.; del Castillo, L. F.; Riande, E. *J. Electrochem. Soc.* **2008**, *155*, F245.
- Fang, J.; Zhai, F.; Guo, X.; Xu, H.; Okamoto, K. J. *Mater. Chem.* **2007**, *17*, 1102.
- Roy, A.; Yu, X.; Dunn, S.; McGrath, J. E. *J. Membr. Sci.* **2009**, *327*, 118.
- Paddison, S. J. *Annu. Rev. Mater. Res.* **2003**, *33*, 289.
- Kreuer, K.-D.; Paddison, S. J.; Spohr, E.; Schuster, M. *Chem. Rev.* **2004**, *104*, 4637.
- Tuckerman, M.; Laasonen, K.; Sprik, M.; Paraniello, M. *J. Chem. Phys.* **1995**, *103*, 150.
- Tuckerman, M.; Laasonen, K.; Sprik, M.; Paraniello, M. *J. Phys. Chem.* **1995**, *99*, 5749.
- Tuckerman, M.; Marx, D.; Klein, M.; Paraniello, M. *Science* **1997**, *275*, 817.
- Marx, D.; Tuckerman, M.; Paraniello, M. *Nature* **1999**, *397*, 601.
- Marx, D.; Tuckerman, M.; Paraniello, M. *J. Phys.: Condens. Matter* **2000**, *12*, A153.
- Spohr, E.; Commer, P.; Kornyshev, A. A. *J. Phys. Chem.* **2002**, *106*, 10560.
- Lobaugh, J.; Voth, G. A. *J. Chem. Phys.* **1996**, *104*, 2056.
- Vuilleumer, R.; Borgis, D. *Chem. Phys. Lett.* **1998**, *284*, 71.
- Vuilleumer, R.; Borgis, D. *J. Chem. Phys.* **1999**, *111*, 4251.
- Schmitt, U. W.; Voth, G. A. *J. Chem. Phys.* **1999**, *111*, 9361.
- Schmitt, U. W.; Voth, G. A. *J. Chem. Phys. Lett.* **2000**, *329*, 36.
- Zahn, D.; Brickmann, J. *Isr. J. Chem.* **1999**, *39*, 469.
- Zahn, D.; Brickmann, J. *Chem. Phys. Lett.* **2000**, *331*, 224.
- Paddison, S. J.; Pratt, L. R.; Zawodzinski, T. A., Jr. *J. Phys. Chem. A* **2001**, *105*, 6226.
- Paddison, S. J.; Paul, R.; Kreuer, K. D. *Phys. Chem. Chem. Phys.* **2002**, *4*, 1151.
- Dokmaïrijan, S.; Spohr, E. *J. Mol. Liq.* **2006**, *129*, 92.
- Cui, S.; Liu, J.; Selvan, M. E.; Keffer, D. J.; Edwards, B. J.; Steele, W. V. *J. Phys. Chem. B* **2007**, *111*, 2208.
- Ennari, J.; Elomaa, M.; Sunholm, F. *Polymer* **1999**, *40*, 5035.
- Ennari, J. *Polymer* **2008**, *49*, 2373.
- Pozuelo, J.; Riande, E.; Saiz, E.; Compañ, V. *Macromolecules* **2006**, *39*, 8862.
- Zhang, H.; Zhou, Y.; Dong, S.; Zhao, Y.; Cui, X.; Wang, H. *Colloid Surf. A: Physicochem. Eng. Asp.* **2009**, *334*, 171.
- Karger, J.; Pfeifer, H.; Heink, W. *Adv. Magn. Reson.* **1998**, *12* (2), 9.
- Callaghan, P. T. *Austr. J. Phys.* **1984**, *237*, 359.
- Zawodzinski, T. A.; Neeman, M.; Sillerud, L. O.; Gottesfeld, S. *J. Phys. Chem.* **1991**, *95*, 6040.
- Jayakody, J. R. P.; Stallworth, P. E.; Mananga, E. S.; Farrington-Zapata, J.; Greenbaum, S. G. *J. Phys. Chem. B* **2004**, *108*, 4260.
- Roy, A.; Hickner, M. A.; Yu, X.; Li, Y.; Glass, T. E.; McGrath, J. E. *J. Polym. Sci., Part B: Polym. Phys.* **2006**, *44*, 2226.
- Zhang, J.; Giotto, V.; Wen, W.-Y.; Jones, A. A. *J. Membr. Sci.* **2006**, *269*, 118.
- Genies, C.; Mercier, R.; Sillion, B.; Cornet, N.; Gebel, G.; Pineri, M. *Polymer* **2001**, *42*, 359.
- Genies, C.; Mercier, R.; Sillion, B.; Petiaud, R.; Cornet, N.; Gebel, G.; Pineri, M. *Polymer* **2001**, *42*, 5097.
- Zhang, Y.; Litt, M.; Savinell, R. F.; Wainright, J. S. *Polym. Prepr. (Am. Chem. Soc., Div. Polym. Chem.)* **1999**, *40* (2), 480.
- Zhang, Y.; Litt, M.; Savinell, R. F.; Wainright, J. S.; Vendramin, J. S. *Polym. Prepr. (Am. Chem. Soc., Div. Polym. Chem.)* **2000**, *41* (2), 1561.
- Gua, X.; Zhai, F.; Fang, J.; Laguna, M. F.; López-González, M.; Riande, E. *J. Phys. Chem. B* **2007**, *111*, 13694.
- Callaghan, P. T.; Jolley, K. W.; Trotter, C. M. *J. Magn. Reson.* **1980**, *39*, 525.
- Materials Studio 3.2, VISUALIZER, AMORPHOUS CELL and DISCOVER modules
- Sun, H.; Mumby, S. J.; Maple, J. R.; Hagler, A. T. *J. Am. Chem. Soc.* **1994**, *116*, 2978.



- (55) Greengard, L.; Rokhlin, V. I. *J. Comput. Phys.* **1987**, 73, 325.
- (56) Ding, H. Q.; Karasawa, N.; Goddard, W. A. *J. Chem. Phys.* **1992**, 97, 4309.
- (57) Ewald, P. P. *Ann. Phys.* **1921**, 64, 253.
- (58) Sun, H. *Macromolecules* **1995**, 28, 701.
- (59) Hill, J.-R.; Sauer, J. *J. Phys. Chem.* **1994**, 98, 1238.
- (60) Maple, J. A.; Hwang, M. J.; Stockfisch, T. P.; Dinur, U.; Waldman, M.; Ewig, C. S.; Hagler, A. T. *J. Comput. Chem.* **1994**, 15, 162.
- (61) Grujicic, M.; Chittajallu, K. M.; Gao, G.; Roy, W. N. *Mater. Sci. Eng.* **2005**, B117, 187.
- (62) Chen, Z.; Gu, Q.; Zou, H.; Zhao, T.; Wang, H. *J. Polym. Sci., Part B: Polym. Phys.* **2007**, 45, 884.
- (63) Rappe, A. K.; Goddard, W. A. *J. Phys. Chem.* **1991**, 95, 3358.
- (64) Stejskal, E. O.; Tanner, J. E. *J. Chem. Phys.* **1965**, 42, 288.
- (65) Muller-Plathé, F. *Acta Polym.* **1994**, 45, 259.
- (66) Ye, G.; Mills, C. M.; Goward, G. R. *J. Membr. Sci.* **2008**, 319, 238.
- (67) Khalfan, A. N.; Sánchez, L. M.; Kodiweera, C.; Greenbaum, S. G.; Bai, Z.; Dang, T. D. *J. Power Sources* **2007**, 173, 853.
- (68) Álvarez-Gallego, Y.; Ruffmann, B.; Silva, V.; Lozano, A. E.; de la Campa, J. G.; Nunes, S. P.; de Abajo, J. *Polymer* **2008**, 49, 3875.
- (69) Waters, J. F.; Likavec, W. R.; Ritchey, W. M. *J. Appl. Polym. Sci.* **1994**, 53, 59.
- (70) Mills, R. *J. Phys. Chem.* **1973**, 77, 688.
- (71) An error was detected in the last column of Table 4 of ref 51. The values of  $D(\text{H}^+)$  collected there are three to four times higher, depending on the water content, than the true values of this parameter.